# Regulation of embryonic neurogenesis by germinal zone vasculature

Mathew Tata[a], Ivan Wall[a,1], Andy Joyce[a], Joaquim M. Vieira[a,2], Nicoletta Kessaris[b], and Christiana Ruhrberg[a,3]

[a]UCL Institute of Ophthalmology, University College London, London EC1V 9EL, United Kingdom; and [b]Wolfson Institute for Biomedical Research, University College London, London WC1E 6BT, United Kingdom

Edited by Sergiu P. Paşca, Stanford University School of Medicine, Stanford, CA, and accepted by Editorial Board Member Solomon H. Snyder October 10, 2016 (received for review August 17, 2016)

**In the adult rodent brain, new neurons are born in two germinal regions that are associated with blood vessels, and blood vessels and vessel-derived factors are thought to regulate the activity of adult neural stem cells. Recently, it has been proposed that a vascular niche also regulates prenatal neurogenesis. Here we identify the mouse embryo hindbrain as a powerful model to study embryonic neurogenesis and define the relationship between neural progenitor cell (NPC) behavior and vessel growth. Using this model, we show that a subventricular vascular plexus (SVP) extends through a hindbrain germinal zone populated by NPCs whose peak mitotic activity follows a surge in SVP growth. Hindbrains genetically defective in SVP formation owing to constitutive NRP1 loss showed a premature decline in both NPC activity and hindbrain growth downstream of precocious cell cycle exit, premature neuronal differentiation, and abnormal mitosis patterns. Defective regulation of NPC activity was not observed in mice lacking NRP1 expression by NPCs, but instead in mice lacking NRP1 selectively in endothelial cells, yet was independent of vascular roles in hindbrain oxygenation. Therefore, germinal zone vascularization sustains NPC proliferation in the prenatal brain.**

blood vessel | neural progenitor | neurogenesis | hindbrain | NRP1

Stem cells are thought to reside within specialized niches that regulate their self-renewal and differentiation via signaling interactions; examples include notch signaling between osteoblasts and hematopoietic stem cells, extracellular matrix (ECM) signaling to epidermal stem cell integrins, and paracrine Wnt signaling across the intestinal crypt-villus axis (1). In the subventricular zone of the lateral ventricles (LV/SVZ) in the adult rodent brain, neural stem cells (NSCs) reside in a specialized niche composed of ependymal cells at the ventricle wall and perigerminal blood vessels (2). LV/SVZ endothelium expresses notch, ephrins, and the neurotrophins PEDF and NT3 to maintain quiescence and pluripotency of the NSCs (3–5), and losing close contact with LV/SVZ vessels therefore increases NSC proliferation (6). Moreover, cultured LV/SVZ-derived NSCs use integrins to attach to laminin-expressing vessels to regulate their mitotic activity (7). The vascular endothelial growth factors (VEGFs) VEGF-A and VEGF-C also contribute to NSC regulation, with the former suggested to promote NSC proliferation through VEGF receptor (VEGFR) VEGFR2 (8) and the latter enhancing neuron production from NSCs through VEGFR3 in the LV/SVZ and hippocampal neurogenic niches (9).

These studies indicate important roles for vascular growth factors, blood vessels, and vessel-derived factors in regulating NSC behavior in the adult mammalian brain. In contrast, how VEGF or blood vessels regulate neurogenesis in the embryonic brain is poorly understood. This is a fundamental question, because despite many similarities, adult and embryonic neurogenesis differ in several respects. Most notably, embryonic neurogenesis arises from an abundant pool of neural progenitor cells (NPCs), which initially proliferate rapidly and then progressively lose their proliferative capacity as they generate a large number of neural progeny with great functional diversity. Moreover, developmental neurogenesis leads to rapid brain growth that necessitates extensive expansion of supporting vasculature, whereas vascular growth is scarce and NSCs proliferate slowly in the adult brain. A recent study suggested that blood vessels alleviate tissue hypoxia in the embryonic dorsal forebrain to promote the commitment of self-renewing NPCs to fate-restricted progenitors (10). Another study suggested that vessels in the ventral forebrain provide anchorage for NPCs that give rise to cortical interneurons (11). Whether blood vessels regulate neurogenesis in other regions of the central nervous system (CNS) is unknown, however.

Neuropilin 1 (NRP1) is a cell surface receptor expressed by blood vessels and NPCs in the embryonic CNS (12, 13). NRP1 promotes CNS vascularization in response to VEGF-A and ECM signals (14, 15) and functions as a VEGF-A and class 3 semaphorin (SEMA3) receptor to regulate neuronal migration and axon guidance (16). Moreover, SEMA3B signals through NRP1 and NRP2 in spinal cord NPCs to orientate their mitotic spindle and regulate the onset of motor neuron differentiation (13). However, it has not yet been examined whether NRP1 acts as a VEGF-A receptor in NPCs, nor is it known whether NRP1-dependent vasculature regulates NPC behavior. Here we show that NRP1 ablation in the mouse embryo hindbrain caused precocious NPC cell cycle exit and therefore premature neural

## Significance

**Neural progenitor cells (NPCs) proliferate to generate precursors for new neurons. To sustain this process, NPCs balance self-renewal with the generation of progeny committed to neuronal differentiation. In the adult mammalian brain, blood vessels and vessel-derived factors help regulate this balance by modulating NPC proliferation and quiescence, independently of vascular roles in providing oxygen and nutrients. In contrast, it has been proposed that vasculature regulates NPC behavior in the developing forebrain by alleviating tissue hypoxia. We show here that germinal zone vasculature in the embryonic hindbrain regulates the balance of NPC self-renewal with neuron production, independently of roles in tissue oxygenation. Information on how blood vessels regulate neurogenesis may aid in the design of therapies for brain regeneration in injury and disease.**

Author contributions: M.T., J.M.V., N.K., and C.R. designed research; M.T., I.W., A.J., and C.R. performed research; N.K. contributed new reagents/analytic tools; M.T. and C.R. analyzed data; and M.T. and C.R. wrote the paper.

The authors declare no conflict of interest.

This article is a PNAS Direct Submission. S.P.P. is a Guest Editor invited by the Editorial Board.

[1]Present address: Department of Biochemical Engineering, University College London, London WC1E 6BT, United Kingdom.

[2]Present address: Department of Physiology, Anatomy, and Genetics, University of Oxford, Oxford OX1 3PT, United Kingdom.

[3]To whom correspondence should be addressed. Email: c.ruhrberg@ucl.ac.uk.

This article contains supporting information online at www.pnas.org/lookup/suppl/doi:10.1073/pnas.1613113113/-/DCSupplemental.

differentiation. This defect was phenocopied in mice lacking NRP1 in endothelial cells but not the NPC lineage, demonstrating an important role for NRP1-dependent germinal zone (GZ) vasculature, rather than VEGF-A signaling through NRP1 in NPCs, in regulating hindbrain neurogenesis. We further found that vasculature regulated NPC self-renewal independently of its role in alleviating tissue hypoxia. Moreover, hindbrains lacking GZ vasculature showed abnormal patterns of NPC mitoses. These findings identify the mouse embryo hindbrain as a powerful model for studying the anatomic and functional relationship of vessel growth and neurogenesis and demonstrate that hindbrain neurogenesis is sustained by an NRP1-dependent vascular niche.

## Results

**Hindbrain NPCs Proliferate Rapidly After a Peak in Vessel Sprouting.** We studied the spatiotemporal relationship of NPC proliferation and CNS vascularization in the developing hindbrain, because its flat architecture is exquisitely suited to visualizing growing vessels near the ventricular surface and NPC mitosis in the ventricular zone (VZ). Thus, whole-mount staining of embryonic day (e) 11.5 hindbrains, corresponding to the 45 somite pair (s) stage (*SI Appendix*, Table S1), identified an isolectin B4 $(IB4)^+$ subventricular vascular plexus (SVP) (12) beneath a layer of phosphohistone H3 $(pHH3)^+$ cells corresponding to mitotic NPCs (Fig. 1 *A* and *B*). Three-dimensional surface rendering demonstrated that filopodia extended from the SVP toward the VZ in gaps between NPCs (Fig. 1*B′*); thus, hindbrain NPCs proliferate near GZ vasculature.

To compare the progression of GZ vascularization and NPC proliferation over time, we performed whole-mount IB4 staining of wild-type (WT) hindbrains from mice on a CD1 genetic background. We observed that only a few vessel sprouts had entered the e9.5/25s hindbrain, but vessel sprouting peaked beneath the VZ at e10.5/35s (Fig. 1 *C* and *D*). Vessel sprouting declined from e11.5/45s onward (Fig. 1 *C* and *D*), when vessel sprouts anastomose to form the SVP (12). Whole-mount $pHH3^+$ staining showed that NPC mitotic activity spanned the period from e9.5/25s to e12.5/50s (Fig. 1*E*) and therefore correlated with the major phase of hindbrain angiogenesis. The peak in NPC mitoses occurred around e11.0/40s, shortly after the peak in vessel sprouting, but declined again after the SVP was established (Fig. 1 *E* and *F*). A small proportion of $pHH3^+$ cells displayed weaker pHH3 staining and formed crescent-shaped pairs (far-right panel in Fig. 1*E*), typical for cells transitioning from anaphase to early telophase (17). These cells, hereafter referred to as anaphase NPCs, typically comprised 20 ± 6.5% of the total mitotic population. The time course of NPC proliferation was similar in C57BL/6 mice, but occurred slightly earlier than in CD1 mice and with a less pronounced peak (Fig. 1*F*). Taken together, these experiments show that vessel sprouting correlates with a surge in NPC mitosis. Therefore, the hindbrain is a suitable model for studying the relationship of NPC proliferation and GZ vasculature in the developing brain.

**Spatial Relationship Between Hindbrain NPCs and Vasculature.** To define the spatial relationship of mouse hindbrain NPCs with GZ vasculature, we examined transverse sections of hindbrains from the avascular stage to the time at which VZ mitotic activity had largely subsided. In contrast to the forebrain, where mitotic NPCs are distributed both at the ventricular surface and in the SVZ, mitotic NPCs in the hindbrain were confined largely to a single layer adjacent to the ventricular wall (Fig. 2*A*). Beneath this layer of mitotic NPCs, BrdU-labeled S-phase NPC nuclei adopted a pseudostratified organization (Fig. 2*A*), suggesting that hindbrain NPCs undergo interkinetic nuclear migration, similar to telencephalic NPCs (18). At e9.5/25s, a small number of radial vessels had invaded the hindbrain from the perineural vascular plexus (PNP) (Fig. 2*A*). At e10.5/35s, radial vessels had sprouted perpendicularly to initiate SVP formation at an average depth of 21.8 ± 1.5 μm from the ventricular surface (Fig. 2*A*). The emerging SVP passed directly through the GZ, and from around e10.5/35s onward, the S-phase NPC nuclei appeared to gather around the SVP (Fig. 2*A*). From e11.5/45s, a deep vessel plexus formed underneath the GZ (Fig. 2*A*). Thus, hindbrain vasculature has a clear anatomic relationship with proliferating NPCs.

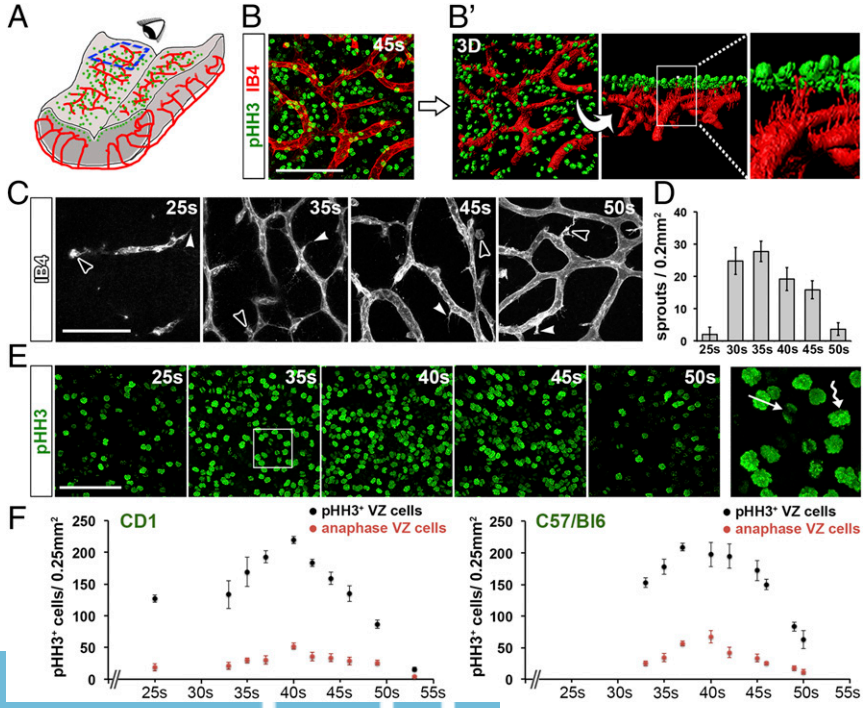


**Fig. 1.** Temporal correlation of blood vessel growth and NPC proliferation in the hindbrain. (*A*) Schematic representation of a flat-mounted e11.5 hindbrain containing mitotic NPCs (green) and blood vessels (red). The blue box indicates the area imaged in *B*, *C*, and *E*; the eye illustrates the observer's point of view. (*B* and *B′*) Proximity of SVP vessels to mitotic NPCs. Maximal projection (*x*, *y*) of a confocal Z-stack (*B*) through flat-mounted e11.5 hindbrains after labeling with the dual vessel and microglia marker IB4 (red) and the mitotic marker pHH3 (green). (Scale bar: 100 μm.) The 3D surface rendering in *B′* illustrates the SVP beneath a layer of mitotic NPCs. The higher magnification of the boxed area shows endothelial cell filopodia projecting between the mitotic NPCs toward the ventricular surface. (*C*–*F*) Time course of vessel sprouting and NPC proliferation in the hindbrain. Maximal projection (*x*, *y*) of confocal Z-stacks through flat-mounted hindbrains at the indicated stages after IB4 labeling, including quantification of vessel sprouts (*C* and *D*) and mitotic and anaphase NPCs in CD1 and C57BL6 backgrounds after pHH3 labeling (*E* and *F*). (Scale bar: 100 μm.) In *C*, examples of vessel sprouts and microglia are indicated with arrowheads and open arrowheads, respectively. The boxed area in *E* is shown at higher magnification to illustrate strongly labeled metaphase NPCs (wavy arrow) and dimly labeled anaphase NPCs (arrow). Data are shown as mean ± SEM; $n \geq 3$ for each time point.

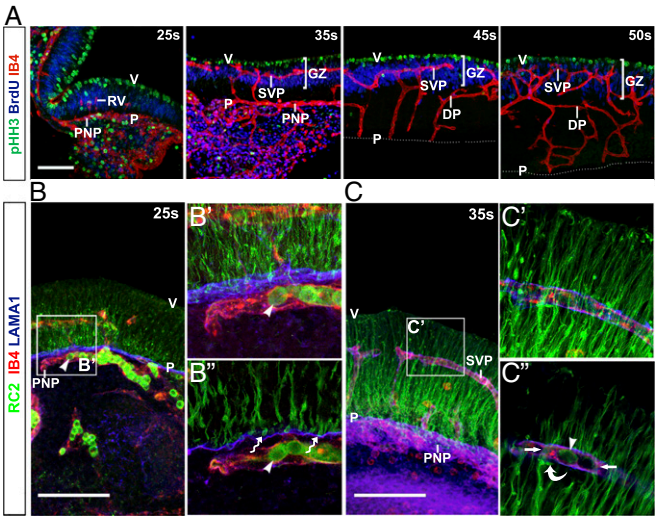


**Fig. 2.** Spatial relationship of blood vessel growth and NPC proliferation in the hindbrain. Confocal Z-stacks of 70-μm transverse sections of WT hindbrains at the indicated stages after a 1-h BrdU pulse after labeling with IB4 together with antibodies for pHH3 and BrdU (*A*) or RC2 and LAMA1 (*B* and *C*). (Scale bar: 20 μm.) The boxed areas in *B* and *C* are shown in higher magnification adjacent to each panel (*B′* and *C′*). Single (1.25 μm) optical sections from these projections are displayed underneath (*B′′* and *C′′*). Arrowheads in *B* and *C* indicate IgM$^+$ blood cells labeled with the secondary antibody used for RC2 detection. The wavy arrow in *B′′* indicates NPC endfeet. Arrows and the curved arrow in *C* denote NPC processes and density near SVP vessels. P, pial surface; V, ventricular surface; RV, radial vessel; DP, deep plexus.

**Hindbrain NPCs Contact the SVP and Vessel-Associated ECM.** The RC2 antibody for the intermediate filament protein nestin visualizes NPC processes in the developing brain (19). RC2 staining was sparse in the hindbrain ventricular region at e9.5/25s, but appeared stronger toward the pial surface (Fig. 2*B* and *SI Appendix*, Fig. S1*A*). At e10.5/35s, RC2$^+$ processes extended from the apical surface toward the pial surface (Fig. 2*C* and *SI Appendix*, Fig. S1*A*). RC2$^+$ endfeet appeared to project onto the laminin-rich basement membrane adjacent to the PNP from e9.5/25s (Fig. 2*B*). Higher magnification showed close apposition of a subset of RC2$^+$ fibers with laminin-coated SVP vessels (Fig. 2*C* and *SI Appendix*, Fig. S1*A′*). At e12.5/50s, toward the end of the neurogenesis period, RC2$^+$ processes were denser in the apical hindbrain (*SI Appendix*, Fig. S1*A*). To visualize the interaction of RC2$^+$ processes from individual NPCs with blood vessels, we performed mosaic labeling with a tamoxifen-inducible *Sox1-iCreER$^{T2}$* transgene and the recombination reporter *Rosa$^{tdTomato/+}$* (*SI Appendix*, *Materials and Methods*). CRE-mediated recombination was detected by immunostaining for the Tomato protein in a subset of NPCs at 35s (*SI Appendix*, Fig. S1*B*). Three-dimensional surface rendering of confocal Z-stacks established that some NPC processes wrapped tightly around GZ vessels (Fig. 3 *A*, *B*, and *D*), whereas others terminated with endfeet on the PNP (Fig. 3 *A* and *C*); therefore, NPCs physically interact with hindbrain vessels.

**NRP1 Regulates the Temporal Pattern of Hindbrain NPC Mitoses.** NRP1 is expressed by hindbrain endothelium and NPCs (12), is essential for hindbrain vascularization (20), and cooperates with NRP2 to regulate SEMA3B-mediated NPC division plane orientation in the spinal cord (13). To determine how NRP1 loss affects GZ vascularization and neurogenesis, we compared stage-matched *Nrp1*-null mutant and control hindbrains. Stage matching was performed to account for a developmental delay caused by NRP1 loss (*SI Appendix*, Table S1 and Fig. S2). Consistent with previous findings (20), radial vessels had entered 32s *Nrp1*-null hindbrains, but failed to branch laterally to form the SVP (Fig. 4*A*). In 40s mutants, occasional vessels had entered the GZ but formed abnormal vascular tufts; other vessels branched laterally beneath the GZ, forming a deep plexus of abnormally large caliber (Fig. 4*A*). Quantification confirmed that the GZ was largely avascular in mutants (Fig. 4*B*). Despite the lack of GZ vasculature, apoptosis was not increased in 32s or 40s *Nrp1*-null hindbrains compared with controls (*SI Appendix*, Fig. S3). Thus, the rudimentary network of radial and deep plexus vessels, combined with an intact PNP and a flat hindbrain architecture, was likely sufficient to maintain hindbrain health during neurogenesis.

GZ organization into a ventricular mitotic NPC layer and a pseudostratified layer of BrdU$^+$ NPC S-phase nuclei was maintained in the mutants (Fig. 4*A*). Moreover, NPC processes in *Nrp1*-null hindbrains extended between the ventricular and pial hindbrain surfaces, suggesting that anchorage to pial ECM was not perturbed; however, there was mild disorganization of NPC processes in some regions lacking vessels (*SI Appendix*, Fig. S4). Furthermore, the GZ of mutant hindbrains appeared thicker at 32s, but thinner at 40s, compared with controls (Fig. 4 *A* and *C*).

Whole-mount imaging of pHH3$^+$ NPCs in the VZ between the 32s and 46s stages suggested an abnormal time course of NPC proliferation in *Nrp1*-null hindbrains, with a premature increase and subsequent decline in the number of mitotic NPCs (Fig. 4 *D* and *E*). Quantification of the number of pHH3$^+$ cells in a detailed time course between 25s and 46s demonstrated that the number of mitotic NPCs remained similar in mutant and control VZ at the 25s stage, when the hindbrain is still largely avascular (Fig. 4*E*). In contrast, the number of pHH3$^+$ NPC figures in the VZ of mutants increased slightly at 32s and prominently at 36s (Fig. 4 *D* and *E*).

Surprisingly, the large increase in the overall number of pHH3$^+$ NPCs in mutants at 36s could be attributed to a transient and striking increase in the number of NPCs in anaphase (Fig. 4 *D* and *E* and *SI Appendix*, Fig. S5), because the number of pHH3$^+$ pre-anaphase NPCs was similar between WT and *Nrp1*-null mutant hindbrains (all pHH3$^+$ mitotic figures minus pHH3$^+$ anaphase figures; *SI Appendix*, Fig. S5). This finding suggests mitotic stalling in the mutant hindbrain at 36s. The proportion of anaphases was again similar in mutants and controls at 40s and 42s, but this apparent normalization was transient as the anaphase phenotype inverted, with the proportion of NPCs in anaphase lower in mutant VZ than in control VZ at the 46s stage (Fig. 4 *D* and *E*). At the 46s stage, when NPC activity begins to subside in WT hindbrains, the overall number of mitotic NPCs was even lower in mutants than controls, indicated by a significantly reduced number of pHH3$^+$ cells in VZ flat mounts (Fig. 4 *D* and *E*), which was confirmed in subsequent analyses by a reduced number of Ki-67$^+$ NPCs in *Nrp1*-null embryos (see below). Therefore, NRP1 is required to ensure a normal pattern of NPC proliferation in the hindbrain and to sustain NPC activity.

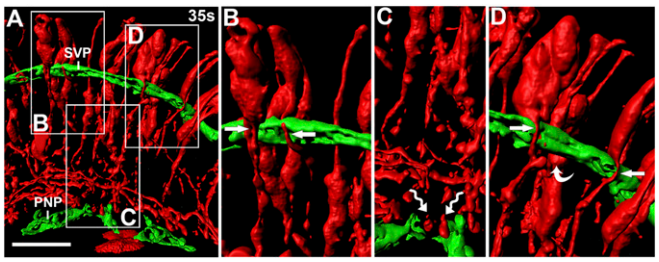


**Fig. 3.** Hindbrain NPC processes contact the SVP. Shown is a 3D surface rendering of confocal Z-stacks of *Sox1-iCreER$^{T2}$;Rosa$^{tdTomato}$* hindbrain sections after labeling for RFP (red) together with IB4 (green). Boxed areas in *A* are shown in higher magnification in *B–D*. Arrows denote NPC processes, wavy arrows indicate NPC endfeet, and the curved arrow indicates an NPC density near blood vessels. (Scale bar: 50 μm.)

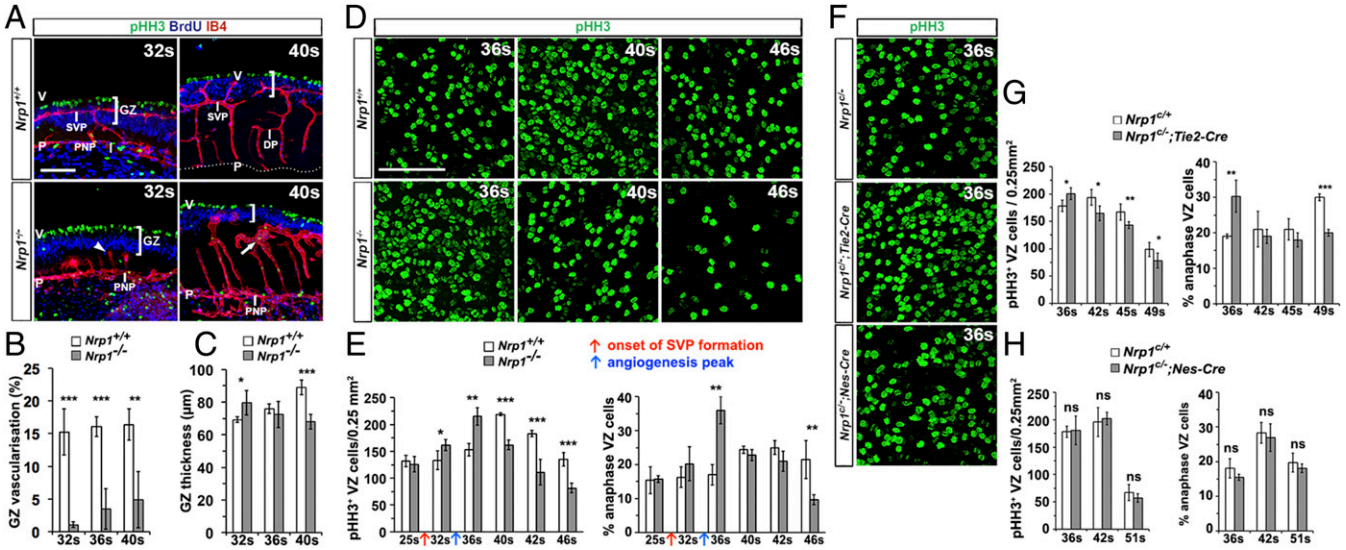


**Fig. 4.** NRP1 regulates hindbrain GZ vascularization and NPC proliferation. (*A–C*) *Nrp1*-null mutants lack GZ vasculature. Maximal projections (*x*, *y*) of confocal Z-stacks from hindbrain sections at the indicated stages after labeling for pHH3 and BrdU together with IB4 (*A*). Brackets denote GZ depth, the arrowhead indicates a dead-ended radial vessel, and the straight arrow indicates an abnormal deep plexus. (Scale bar: 100 μm.) P, pial surface; V, ventricular surface; DP, deep plexus. (*B* and *C*) Quantification of GZ vascular coverage as $IB4^+$ per $BrdU^+$ GZ area (*B*) and GZ thickness as average depth of the $BrdU^+$ GZ area (*C*). (*D–H*) Abnormal NPC proliferation in *Nrp1* mutants. Maximal projection (*x*, *y*) of confocal Z-stacks of flat-mounted WT vs. *Nrp1*-null (*D*) and $Nrp1^{c/+}$ control vs. *Tie2-Cre;*$Nrp1^{c/-}$ or *Nes-Cre;*$Nrp1^{c/-}$ (*F*) hindbrain VZ at the indicated stages after pHH3 labeling. Quantification of $pHH3^+$ NPCs in the VZ, including proportion of NPCs in anaphase, per 0.25 $mm^2$ VZ at the indicated stages for constitutive (*E*) or cell type-selective (*G* and *H*) *Nrp1*-null and stage-matched control hindbrains. In *E*, red and blue arrows indicate the onset of SVP formation and peak vessel sprouting in WT hindbrains, respectively. Data in all graphs are mean ± SEM; $n \geq 3$ for each time point and genotype. $^*P < 0.05$; $^{**}P < 0.01$; $^{***}P < 0.001$.

**NRP1 Regulates NPC Division Through Its Role in Vessel Growth.** To distinguish whether NRP1-dependent blood vessels or NRP1 signaling in NPCs regulate hindbrain neurogenesis, we analyzed *Tie2-Cre*;$Nrp1^{c/-}$ and *Nes-Cre*;$Nrp1^{c/-}$ mutant mice, which were previously shown to lack NRP1 in the endothelial lineage and the neural lineage, respectively (20). *Nes-Cre*;$Nrp1^{c/-}$ mutants have normal hindbrain vascularization; in contrast, *Tie2-Cre*;$Nrp1^{c/-}$ mutants have vascular defects similar to, but milder than, those of full NRP1 knockouts, owing to the persistence of a few recombination-resistant endothelial cells that enable low-level vessel sprouting (20). We found that *Tie2-Cre*;$Nrp1^{c/-}$ mutants had an avascular GZ at 32s, but GZ vascularization had partially recovered at 48s (*SI Appendix*, Fig. S6*A*). As observed in constitutive *Nrp1*-null mutants, NPC processes extended between the ventricular and pial surfaces in *Tie2-Cre*;$Nrp1^{c/-}$ hindbrains, but there was mild disorganization of NPC processes in some regions lacking vessels (*SI Appendix*, Fig. S6*B*).

Quantification demonstrated that *Tie2-Cre*;$Nrp1^{c/-}$ mutant VZ had an abnormal pattern of $pHH3^+$ NPC mitoses, including a greater proportion of anaphase NPCs than control VZ at 36s and significantly less NPC mitosis thereafter (Fig. 4 *F* and *G*). Thus, endothelial *Nrp1*-null mutants have an NPC mitosis defect similar to that of constitutive *Nrp1*-null mutants. However, the defect was milder in endothelial compared with full NRP1-null mutants (compare Fig. 4*E* and Fig. 4*G*), correlating with a milder defect in GZ vascularization (compare Fig. 4*A* and *SI Appendix*, Fig. S6*A*). In contrast, *Nes-Cre*;$Nrp1^{c/-}$ mutant hindbrains had a similar number of NPC mitoses compared with controls at all stages examined (Figs. 4 *F* and *H*; somite counting excluded a developmental delay in *Nes-Cre*;$Nrp1^{c/-}$ mutants).

Given that VEGFR2 (FLK) is an alternative VEGF-A receptor expressed in NPCs derived from embryonic telencephalon (21), we asked whether it might compensate for NRP1 in hindbrain NPCs. NPCs did not obviously express VEGFR2, however (*SI Appendix*, Fig. S7). The lack of VEGFR2 expression in hindbrain NPCs, together with a normal number of NPC mitoses in *Nes-Cre*;$Nrp1^{c/-}$ mutants, suggests that VEGF-A is unlikely to directly regulate NPC proliferation during hindbrain neurogenesis. Instead, NRP1-dependent GZ vasculature regulates hindbrain neurogenesis.

**Hindbrain Vasculature Promotes NPC Self-Renewal Independently of Tissue Oxygenation.** Whereas pHH3 staining had suggested cell cycle stalling in mitosis at the 36s stage when GZ vessel sprouting peaks, NPC mitotic behavior was only subtly affected at 32s, when blood vessels first enter the GZ to form the SVP (Fig. 4). Therefore, we performed additional experiments at 32s to examine whether GZ vascularization helps sustain the proliferative capacity of NPCs. We injected pregnant dams with BrdU at 24 h before isolating 32s hindbrains and then performed immunolabeling with antibodies for BrdU and the proliferation marker Ki-67 (Fig. 5*A*). NPCs that had undergone terminal divisions after the BrdU injection would be labeled with BrdU only, whereas self-renewing NPCs (i.e., cells that continued to cycle) would be double-positive for BrdU and Ki-67 (22). Strikingly, 25% fewer NPCs were double-positive in *Nrp1*-null compared with control hindbrains (Fig. 5 *B* and *C*). This decrease in cycling NPCs was inversely correlated with a larger area labeled with TUJ1, a marker for postmitotic neurons (Fig. 5 *B* and *C*); therefore, an increased proportion of NPCs undergoes cell cycle exit at 32s. Moreover, this analysis demonstrated ectopic neuronal differentiation in the VZ of mutants (Fig. 5*B*). Similar, but milder, defects in NPC self-renewal were observed in embryos selectively lacking endothelial NRP1 (Fig. 5 *B* and *C*). Accordingly, a substantial proportion of NPCs undergoes precocious and incorrectly placed neurogenesis in hindbrains failing to establish GZ vasculature owing to NRP1 deficiency.

Interestingly, even though the absolute number of $Ki\text{-}67^+$ cycling NPCs had decreased significantly by 46s (*SI Appendix*, Fig. S8*A*), the relative proportion of $Ki\text{-}67^+$ cycling NPCs in all $BrdU^+$ NPCs was similar in *Nrp1*-null mutant and control hindbrains at this stage (*SI Appendix*, Fig. S8*B*). However, regaining this equilibrium between cycling and differentiating NPCs at this late

DEVELOPMENTAL BIOLOGY

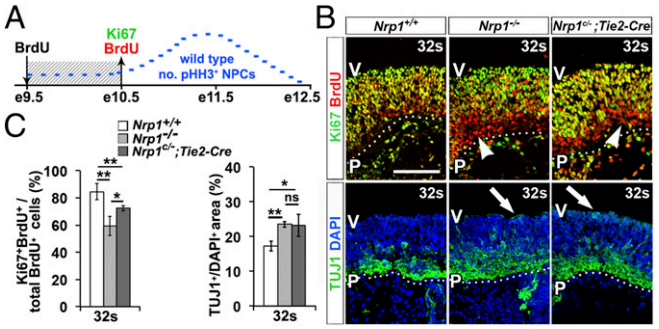


**Fig. 5.** Premature neurogenesis in constitutive and endothelial *Nrp1*-null hindbrains. (*A*) Schematic representation of BrdU labeling. Embryos received BrdU on e9.5 and were analyzed on e10.5. The blue line represents the pattern of NPC mitosis during hindbrain neurogenesis. (*B*) Ten-micrometer transverse sections from 32s hindbrains of the indicated genotypes were labeled for BrdU and Ki-67 or with TUJ1 and the nuclear counterstain DAPI. (Scale bar: 20 μm.) Dotted lines demarcate the basal hindbrain surface. Arrowheads indicate examples of Ki-67$^-$/BrdU$^+$ cells; arrows denote ectopic TUJ1 staining in the VZ. P, pial surface; V, ventricular surface. (*C*) Proportion of Ki-67$^+$BrdU$^+$ in all BrdU$^+$ cells and neuronal differentiation measured as TUJ1$^+$/DAPI$^+$ area. Data are expressed as mean ± SEM; $n \geq 3$ for each genotype and time point. ns, not significant ($P \geq 0.05$); *$P < 0.05$; **$P < 0.01$.

stage in the course of neurogenesis had failed to avert the overall loss of NPC proliferative capacity for hindbrain growth, because hindbrain depth along the apicobasal axis and cross-sectional hindbrain area were significantly reduced at 46s in mutants compared with controls (*SI Appendix*, Fig. S8 *C* and *D*). Taken together, the observations suggest that the NPC pool was prematurely depleted in hindbrains lacking GZ vasculature, with severe consequences for hindbrain growth.

We next examined whether increased tissue hypoxia due to vascular insufficiency was responsible for these neurogenesis defects. Premature cell cycle exit occurred at a time when the hindbrain was less oxygenated in *Nrp1*-null mutants compared with controls, as demonstrated by increased expression of the hypoxia-induced genes *Hif1a* and *Vegfa* and higher protein levels of the hypoxia-responsive glucose transporter GLUT1 (*SI Appendix*, Fig. S9 *A*, *C*, and *D*). Housing pregnant dams in an 80% oxygen atmosphere for 24 h before embryo collection (10) restored hindbrain oxygenation, but failed to rescue the self-renewal and neuronal differentiation defects in NRP1-null hindbrains (*SI Appendix*, Fig. S9 *B*–*D*). Therefore, GZ vasculature regulates hindbrain neurogenesis independently of its role in tissue oxygenation.

## Discussion

Here we have identified the mouse embryo hindbrain as a powerful model for studying neurogenesis with unique advantages. These include the ability to capture the extent and prevalence of organ-wide NPC mitoses in flat-mounted VZ for quantitative analysis and to study a proliferating neuroepithelium in which most NPC mitoses are confined to a region immediately adjacent to the ventricular surface. Moreover, we were able to take advantage of established genetic mouse models to distinguish the possible action of NRP1 in hindbrain NPCs as a receptor for ligands such as VEGF-A from its indirect role in regulating hindbrain neurogenesis through a role in blood vessel patterning. We found that NRP1 expression by endothelial cells, but not by NPCs, was required to regulate NPC mitotic behavior (Fig. 4).

Previous in vitro studies have shown that NPCs in neurospheres derived from e14 forebrain expressed VEGFR2, and that exogenous VEGF-A increased neurosphere number and cell survival (21). However, another forebrain study found that VEGFR2 is endogenously expressed in the endothelial cells of the embryonic brain, but not in nonendothelial cells such as NPCs (23). In agreement with the latter study, we did not detect obvious VEGFR2 expression in the hindbrain VZ (*SI Appendix*, Fig. S7); thus, it appears unlikely that NRP1 or VEGFR2 conveys VEGF-A signals to regulate hindbrain NPC proliferation. We have not investigated whether NRP1 in hindbrain NPCs cooperates with NRP2 to convey semaphorin signals for mitotic spindle orientation, as reported for the spinal cord (13), because the NPC defect that we describe here could be attributed to defective NRP1 signaling in endothelial cells, rather than to cell-autonomous NRP1 signaling in NPCs (Fig. 4). Thus, our findings in the mouse embryo hindbrain agree with those in the adult brain, which demonstrate that vasculature sustains NSC proliferation (3–5, 24).

Hindbrain NPC mitosis normally peaks at the time when angiogenic sprouting is maximal in the GZ and begins to subside once sprouts fuse into the SVP that provides the GZ vasculature (Figs. 1 and 2). In agreement with a functional role of GZ vasculature in regulating hindbrain neurogenesis, we observed that a considerable proportion of hindbrain NPCs underwent premature cell cycle exit in both constitutive and endothelial-specific *Nrp1*-null mutants lacking GZ vasculature (Fig. 5). Subsequently, a proportion of those NPCs that had not exited the cell cycle by the 32s stage showed abnormal mitotic NPC behavior in both constitutive and endothelial-specific *Nrp1*-null mutants lacking GZ vasculature. In particular, the proportion of NPCs in anaphase among all mitotic NPCs was increased in these mutants at a time when GZ vasculature is normally established, but was lacking in mutants (Fig. 4 and *SI Appendix*, Fig. S5). Prolonged mitosis has been reported to skew the fate of dividing NPCs toward the generation of neurons at the expense of generating further NPCs (25). Therefore, given the combined defects in excessive NPC cell cycle exit at 32s and mitotic NPC stalling at 36s in *Nrp1* mutants lacking GZ vasculature, it was not surprising to find that the pool of cycling progenitors was considerably depleted by the 46s stage, when hindbrain growth was accordingly severely compromised (*SI Appendix*, Fig. S8).

We cannot currently explain why some NPCs in *Nrp1* mutant hindbrains undergo a precocious cell cycle exit at 32s while others continue to cycle beyond the 32s stage only to stall in anaphase, nor do we know why anaphase stalling at 36s reverses into accelerated anaphase transition at 46s in *Nrp1* mutants lacking GZ vasculature. One possible explanation for why a loss of GZ vasculature may affect NPC behavior differently at successive developmental stages may be that specific NPC subsets change their responsiveness to multiple, overlapping extrinsic signals over time. In analogy, it has been observed that sonic hedgehog signals increase S-phase length in spinal motor neuron progenitors as brain development progresses, with a prolonged S-phase and thus a longer cell cycle time in self-renewing NPCs in younger embryos (26). Alternatively, distinct subsets of NPCs, generated in consecutive phases and acting as progenitors for different neural or glial subtypes, may respond differently to vessel-derived cues, as has been reported for interneuron-committed NPCs in the ventral forebrain (11). Importantly, our observations suggest that the hindbrain model is exquisitely suited for identifying how extrinsic factors regulate the behavior of changing NPC populations over time.

The anatomic relationship of NPCs and GZ vasculature in the hindbrain is reminiscent of that recently described for the forebrain, where NPCs and their processes also cluster around vessels (11, 23, 27). Moreover, loss of GZ vasculature increased hypoxia in the hindbrain (*SI Appendix*, Fig. S9), as was recently reported for the forebrain (10). Interestingly, tissue hypoxia in the dorsal forebrain impaired NPC commitment toward neuronal specification (10). In contrast to the forebrain, however, we observed increased NPC commitment and neural differentiation in hindbrains lacking GZ vasculature (Fig. 5). Moreover, a hypoxic insult was not the obvious cause of the observed hindbrain

NPC defect, given that NPC self-renewal and premature neuronal differentiation were not rescued by restoration of tissue oxygenation (*SI Appendix*, Fig. S9). Therefore, the *Nrp1*-null mutant hindbrain provides a mammalian model suited for determining the role of GZ vasculature in neurogenesis independent of the general role of blood vessels in maintaining tissue oxygenation.

The different requirements for blood vessels identified in the previous forebrain study and our present work on hindbrain neurogenesis may reflect differences in the NPC subtypes present in these organs; $TBR2^+$ basal progenitors are abundant in the forebrain, but are not found in the hindbrain (28). Alternatively, or additionally, the different neurogenesis defects observed in the forebrain and hindbrain studies may be explained by the use of different mouse models. In particular, NRP1-deficient hindbrains specifically lack GZ vasculature, but contain patent vasculature in other hindbrain areas (Fig. 4) (20), whereas the forebrain vasculature in GPR124 mutants is severely hemorrhagic and thus likely leaky and poorly functional (29). Moreover, a low level of apoptosis in the *Nrp1*-deficient hindbrain (*SI Appendix*, Fig. S3) may be explained in part by the hindbrain's uniquely flat architecture, which instills proximity of tissue components to the PNP plexus and cerebrospinal fluid for nourishment.

In summary, we have shown here that hindbrain GZ vasculature provides essential extrinsic signals above and beyond its role in tissue oxygenation to modulate the NPC cell cycle and thereby sustain neurogenesis. Taken together with the recent forebrain studies identifying oxygen-dependent regulation of NPC commitment, our findings identify GZ vasculature as a crucial component of the embryonic niche for neurogenesis, with region-specific roles in regulating NPC fate and the onset of neuronal differentiation. Whether the previously discovered functions of blood vessels in paracrine or contact-dependent modulation of adult NSCs also operate in the embryonic hindbrain NPC niche remains unclear. Our observations that angiogenesis and neurogenesis proceed in overlapping spatiotemporal windows (Figs. 1 and 2), and that hindbrain (Fig. 3) and ventral forebrain (11) NPC processes seemingly wrap around GZ vessels, are certainly consistent with both possibilities. Importantly, however, it cannot be assumed that specific molecules operating in the adult neurogenic niche have similar roles in the embryo. Accordingly, differences in the extrinsic regulation of adult and embryonic neurogenesis are plentiful (30), as exemplified by the opposing roles of niche-derived signals, such as NT3, in mediating quiescence of adult NSCs (4) versus the commitment of embryonic NPCs to neuronal differentiation (31). Thus, future work might exploit the unique advantages of the hindbrain model to organ-wide imaging and quantitative analysis to identify the signaling mechanisms underlying the vascular regulation of NPC maintenance and differentiation in the developing mammalian brain.

## Materials and Methods

All animal work was carried out in accordance with U.K. Home Office and local ethical guidelines. *Nrp1*-null CD1 mice and endothelial- or NPC-specific NRP1-null C57/Bl6 mice have been described previously (15, 20). *Sox1-iCreER$^{T2}$* mice were developed by N.K. and crossed to *Rosa$^{tdTomato}$* reporter mice (32). To obtain embryos of defined developmental stages, mice were paired overnight, and the day of discovery of a copulation plug was designated embryonic day (e) 0.5. In some experiments, pregnant females were injected intraperitoneally with 10 mg/kg BrdU. Dissected hindbrains were immunostained as described previously (33), and the number of proliferating NPCs was quantified by manual counting. To determine whether two datasets were significantly different, we used a two-tailed, unpaired *t* test. Further details are provided in *SI Appendix, Materials and Methods*.

**ACKNOWLEDGMENTS.** We thank U. Dennehy, M. Daglish, A. Fantin, L. Denti, and the staff of the Biological Resources Unit and Imaging Facility of the UCL Institute of Ophthalmology for technical help. We also thank W. D. Richardson for contributions to generating *Sox1-iCreER$^{T2}$* mice and M. Golding, F. Guillemot, and F. Doetsch for valuable advice. This study was supported by Wellcome Trust PhD Studentship 096621/Z/11/Z (to M.T.) and Investigator Award 095623/Z/11/Z (to C.R.), Medical Research Council Grants G0601093 (to C.R.) and G0800575 (to W.D.R and N.K.), and European Research Council Starting Grant 207807 (to N.K.).

1. Li L, Xie T (2005) Stem cell niche: Structure and function. *Annu Rev Cell Dev Biol* 21: 605–631.
2. Tavazoie M, et al. (2008) A specialized vascular niche for adult neural stem cells. *Cell Stem Cell* 3(3):279–288.
3. Ottone C, et al. (2014) Direct cell-cell contact with the vascular niche maintains quiescent neural stem cells. *Nat Cell Biol* 16(11):1045–1056.
4. Delgado AC, et al. (2014) Endothelial NT-3 delivered by vasculature and CSF promotes quiescence of subependymal neural stem cells through nitric oxide induction. *Neuron* 83(3):572–585.
5. Andreu-Agulló C, Morante-Redolat JM, Delgado AC, Fariñas I (2009) Vascular niche factor PEDF modulates Notch-dependent stemness in the adult subependymal zone. *Nat Neurosci* 12(12):1514–1523.
6. Niola F, et al. (2012) Id proteins synchronize stemness and anchorage to the niche of neural stem cells. *Nat Cell Biol* 14(5):477–487.
7. Shen Q, et al. (2008) Adult SVZ stem cells lie in a vascular niche: A quantitative analysis of niche cell-cell interactions. *Cell Stem Cell* 3(3):289–300.
8. Jin K, et al. (2002) Vascular endothelial growth factor (VEGF) stimulates neurogenesis in vitro and in vivo. *Proc Natl Acad Sci USA* 99(18):11946–11950.
9. Calvo CF, et al. (2011) Vascular endothelial growth factor receptor 3 directly regulates murine neurogenesis. *Genes Dev* 25(8):831–844.
10. Lange C, et al. (2016) Relief of hypoxia by angiogenesis promotes neural stem cell differentiation by targeting glycolysis. *EMBO J* 35(9):924–941.
11. Tan X, et al. (2016) Vascular influence on ventral telencephalic progenitors and neocortical interneuron production. *Dev Cell* 36(6):624–638.
12. Fantin A, et al. (2010) Tissue macrophages act as cellular chaperones for vascular anastomosis downstream of VEGF-mediated endothelial tip cell induction. *Blood* 116(5):829–840.
13. Arbeille E, et al. (2015) Cerebrospinal fluid-derived Semaphorin3B orients neuroepithelial cell divisions in the apicobasal axis. *Nat Commun* 6:6366.
14. Raimondi C, et al. (2014) Imatinib inhibits VEGF-independent angiogenesis by targeting neuropilin 1-dependent ABL1 activation in endothelial cells. *J Exp Med* 211(6): 1167–1183.
15. Fantin A, et al. (2015) NRP1 regulates CDC42 activation to promote filopodia formation in endothelial tip cells. *Cell Rep* 11(10):1577–1590.
16. Mackenzie F, Ruhrberg C (2012) Diverse roles for VEGF-A in the nervous system. *Development* 139(8):1371–1380.
17. Hans F, Dimitrov S (2001) Histone H3 phosphorylation and cell division. *Oncogene* 20(24):3021–3027.
18. Sauer F (1935) Mitosis in the neural tube. *J Comp Neurol* 62(2):377–405.
19. Haubst N, Georges-Labouesse E, De Arcangelis A, Mayer U, Götz M (2006) Basement membrane attachment is dispensable for radial glial cell fate and for proliferation, but affects positioning of neuronal subtypes. *Development* 133(16):3245–3254.
20. Fantin A, et al. (2013) NRP1 acts cell autonomously in endothelium to promote tip cell function during sprouting angiogenesis. *Blood* 121(12):2352–2362.
21. Wada T, et al. (2006) Vascular endothelial growth factor directly inhibits primitive neural stem cell survival but promotes definitive neural stem cell survival. *J Neurosci* 26(25):6803–6812.
22. Arnold SJ, et al. (2008) The T-box transcription factor Eomes/Tbr2 regulates neurogenesis in the cortical subventricular zone. *Genes Dev* 22(18):2479–2484.
23. Javaherian A, Kriegstein A (2009) A stem cell niche for intermediate progenitor cells of the embryonic cortex. *Cereb Cortex* 19(Suppl 1):i70–i77.
24. Crouch EE, Liu C, Silva-Vargas V, Doetsch F (2015) Regional and stage-specific effects of prospectively purified vascular cells on the adult V-SVZ neural stem cell lineage. *J Neurosci* 35(11):4528–4539.
25. Pilaz LJ, et al. (2016) Prolonged mitosis of neural progenitors alters cell fate in the developing brain. *Neuron* 89(1):83–99.
26. Saade M, et al. (2013) Sonic hedgehog signaling switches the mode of division in the developing nervous system. *Cell Reports* 4(3):492–503.
27. Stubbs D, et al. (2009) Neurovascular congruence during cerebral cortical development. *Cereb Cortex* 19(Suppl 1):i32–i41.
28. Kwon GS, Hadjantonakis AK (2007) Eomes::GFP—a tool for live imaging cells of the trophoblast, primitive streak, and telencephalon in the mouse embryo. *Genesis* 45(4): 208–217.
29. Kuhnert F, et al. (2010) Essential regulation of CNS angiogenesis by the orphan G protein-coupled receptor GPR124. *Science* 330(6006):985–989.
30. Urbán N, Guillemot F (2014) Neurogenesis in the embryonic and adult brain: Same regulators, different roles. *Front Cell Neurosci* 8:396.
31. Parthasarathy S, Srivatsa S, Nityanandam A, Tarabykin V (2014) Ntf3 acts downstream of Sip1 in cortical postmitotic neurons to control progenitor cell fate through feedback signaling. *Development* 141(17):3324–3330.
32. Madisen L, et al. (2010) A robust and high-throughput Cre reporting and characterization system for the whole mouse brain. *Nat Neurosci* 13(1):133–140.
33. Fantin A, Vieira JM, Plein A, Maden CH, Ruhrberg C (2013) The embryonic mouse hindbrain as a qualitative and quantitative model to study the molecular and cellular mechanisms of angiogenesis. *Nat Protoc* 8(2):418–429.